Plasma filament investigation by transverse optical interferometry and terahertz scattering

Sergey Bodrov,[1,2,*] Vladimir Bukin,[3] Maxim Tsarev,[2,1] Aleksey Murzanev,[1] Sergey Garnov,[3] Nickolay Aleksandrov,[4] and Andrey Stepanov[1]

[1]Institute of Applied Physics, Russian Academy of Sciences, 46 Ulyanov Street, Nizhny Novgorod, 603950 Russia
[2]University of Nizhny Novgorod, 23 Gagarin Avenue, Nizhny Novgorod, 603950 Russia
[3]Prokhorov General Physics Institute, Russian Academy of Sciences, 38 Vavilov Street, Moscow, 119991 Russia
[4]Moscow Institute of Physics and Technology, Institutski proezd, 9, Dolgoprudny, Moscow region, 141700 Russia
bosbor@ufp.appl.sci-nnov.ru

Abstract: Transverse plasma distribution with 10^{17} cm^{-3} maximum electron density and 150 μm transverse size in a plasma filament formed in air by an intense femtosecond laser pulse was measured by means of optical interferometry. Two orders of magnitude decay of the electron density within 2 ns was obtained by combined use of the interferometry and newly proposed terahertz scattering techniques. Excellent agreement was obtained between the measured plasma density evolution and theoretical calculation.

OCIS codes: (190.7110) Ultrafast nonlinear optics; (280.5395) Plasma diagnostics; (120.3180) Interferometry; (120.5820) Scattering measurements; (040.2235) Far infrared or terahertz.

References and links

1. A. Couairon, and A. Mysyrowicz, "Femtosecond filamentation in transparent media," Phys. Rep. **441**(2-4), 47–189 (2007).
2. L. Bergé, S. Skupin, R. Nuter, J. Kasparian, and J.-P. Wolf, "Ultrashort filaments of light in weakly ionized, optically transparent media," Rep. Prog. Phys. **70**(10), 1633–1713 (2007).
3. F. Théberge, W. Liu, P. Tr. Simard, A. Becker, and S. L. Chin, "Plasma density inside a femtosecond laser filament in air: strong dependence on external focusing," Phys. Rev. E Stat. Nonlin. Soft Matter Phys. **74**(3), 036406 (2006).
4. J. Yu, D. Mondelain, J. Kasparian, E. Salmon, S. Geffroy, C. Favre, V. Boutou, and J. P. Wolf, "Sonographic probing of laser filaments in air," Appl. Opt. **42**(36), 7117–7120 (2003).
5. S. Tzortzakis, B. Prade, M. Franco, and A. Mysyrowicz, "Time-evolution of the plasma channel at the trail of a self-guided IR femtosecond laser pulse in air," Opt. Commun. **181**(1-3), 123–127 (2000).
6. J. Liu, Z. Duan, Z. Zeng, X. Xie, Y. Deng, R. Li, Z. Xu, and S. L. Chin, "Time-resolved investigation of low-density plasma channels produced by a kilohertz femtosecond laser in air," Phys. Rev. E Stat. Nonlin. Soft Matter Phys. **72**(2), 026412 (2005).
7. C. Y. Chien, B. La Fontaine, A. Desparois, Z. Jiang, T. W. Johnston, J. C. Kieffer, H. Pépin, F. Vidal, and H. P. Mercure, "Single-shot chirped-pulse spectral interferometry used to measure the femtosecond ionization dynamics of air," Opt. Lett. **25**(8), 578–580 (2000).
8. M. Takeda, H. Ina, and S. Kobayashi, "Fourier-transform method of fringe-pattern analysis for computer-based topography and interferometry," J. Opt. Soc. Am. **72**(1), 156–160 (1982).
9. A. Stepanov, N. Bochkarev, and A. Kabanov, "Spatial localization of the region of filamentation along the trace of propagation of focused femtosecond laser radiation in air," Atmosphere. Oceanic Opt. J. **20**, 859–862 (2007).
10. I. A. Kossyi, A. Yu. Kostinsky, A. A. Matveyev, and V. P. Silakov, "Kinetic scheme of the non-equilibrium discharge in nitrogen-oxygen mixtures," Plasma Sources Sci. Technol. **1**(3), 207–220 (1992).
11. F. J. Mehr, and M. A. Biondi, "Electron temperature dependence of recombination of O2+ and N2+ ions with electrons," Phys. Rev. **181**(1), 264–271 (1969).
12. L. M. Biberman, V. S. Vorobyev, and I. T. Yakubov, *Kinetics of Nonequilibrium Low-Temperature Plasma* (Nauka, Moscow, 1982 in Russian) [(Consultants Bureau, New York, 1987 in English)].
13. N. L. Aleksandrov, S. V. Kindysheva, M. M. Nudnova, and A. Yu. Starikovskiy, "Mechanism of ultra-fast heating in a non-equilibrium weakly ionized air discharge plasma in high electric fields," J. Phys. D Appl. Phys. **43**(25), 255201 (2010).
14. N. A. Dyatko, I. V. Kochetov, A. P. Napartovich, and A. G. Sukharev, EEDF: the software package for calculations of the electron energy distribution function in gas mixtures. *http://www.lxcat.laplace.univ-tlse.fr/software/EEDF/*
15. A. I. Florescumitchell, and J. B. A. Mitchell, "Dissociative recombination," Phys. Rep. **430**(5-6), 277–374 (2006).

#142643 - $15.00 USD Received 15 Feb 2011; revised 12 Mar 2011; accepted 14 Mar 2011; published 24 Mar 2011

1. Introduction

Filamentation of intense femtosecond laser pulses was first observed in experiments about 15 years ago and has become a field of intense research activity [1, 2]. One of the key roles in the filamentation is played by the laser induced plasma which stops self-focusing of the laser beam. Dynamical balance between self-focusing and plasma defocusing results in creation of a long plasma channel and laser pulse propagation with suppressed diffraction that is attractive to possible practical applications, such as remote sensing or lightning control.

Several approaches to measuring plasma density and plasma decay were reported in the literature. In the fluorescence technique, a fluorescent signal is assumed to be, up to calibration function, a measure of plasma density [3]. An acoustic technique was proposed to measure relative longitudinal distribution of plasma density [4]. Electric measurement of plasma conductivity was used to infer on the evolution of electron density on a time scale larger than nanoseconds [5]. Time-resolved transverse [5] and longitudinal [3,6] diffractometry techniques allow measuring plasma density with picosecond resolution, but with some assumptions on plasma density distribution. In longitudinal diffractometry, plasma density is averaged along the length of a plasma channel. Direct measurement of plasma density without additional assumptions and picosecond resolution can be realized by the transverse interferometric technique, but because of a small transverse size of the plasma filament (~100 μm) this approach was, up to now, demonstrated only for high plasma densities (~10^{18} cm^{-3}) obtained in a laser spark for tightly focused laser radiation [7].

In this paper, we present direct experimental measurements of spatial distribution of plasma density and plasma decay in a single-filament regime by two complimentary techniques. Using highly sensitive (~λ/1000) transverse optical interferometry, we measured a plasma density profile in a filament from the moment of ionization to 0.3 ns after ionization. The corresponding peak electron density was shown to experience decay from 9×10^{16} cm^{-3} to 2×10^{16} cm^{-3}. To measure lower plasma densities over longer time intervals, we propose (for the first time to the best of our knowledge) the technique of transverse terahertz scattering of pulsed THz radiation from the filament. In our experiment, we demonstrated applicability of the technique for plasma density decay measurements down to 10^{15} cm^{-3} at 2 ns. A model which adequately describes plasma decay by accounting for dissociative and three-body recombination, recombination of electrons with complex ions, cooling and heating of electrons was developed.

2. Experimental setup

A Ti:Sapphire laser system generating 60-fs FWHM laser pulses at 795 nm central wavelength with 10 Hz repetition rate was used to create and to probe plasma filament. The system provided the energy in the laser pulse up to 10 mJ. The radius of the beam was 5 mm (at $1/e^2$). The laser pulse was focused in ambient air at atmospheric pressure by a 125 cm focal length spherical mirror (S.M., see Fig. 1). The plasma filament was formed near the focal plane. The observed length of the plasma channel was 1-10 cm, depending on the laser pulse energy. Part (about ¼ in energy) of the laser pulse was split from the main (pump) pulse before focusing and used as a probe pulse (Fig. 1). To investigate plasma density in the filament and its temporal evolution we used two techniques: transverse optical interferometry (the 1st setup in Fig. 1) and transverse pulsed terahertz scattering (the 2nd setup in Fig. 1). In transverse optical interferometry, the probe pulse after passing a delay line traversed the plasma filament perpendicularly. Then it was split into two parts in a Michelson interferometer and formed an interferometric image on a CCD camera placed in one of the arms of the interferometer. A 7x telescope in front of the interferometer was used to obtain better spatial resolution.

In the newly proposed transverse pulsed terahertz scattering technique the probe laser pulse (after the delay line) generated a pulse of THz radiation in a 1-mm thick ZnTe crystal. The pulse duration was ~1 ps with the maximum of the spectrum near 1 THz (inset in Fig. 1). Visible dips in the spectrum are a result of water vapor absorption. The THz pulse was

#142643 - $15.00 USD Received 15 Feb 2011; revised 12 Mar 2011; accepted 14 Mar 2011; published 24 Mar 2011

focused on the plasma filament by an off-axis parabola with focal length F = 5 cm (Fig. 1). Terahertz radiation scattered from the plasma in the perpendicular direction (90° scattering angle) was focused by a teflon lens (F = 4 cm, D = 4 cm) and collected by a liquid-He-cooled InSb hot electron bolometer (QMS Instruments, model QFI/4). Plasma density value was found from the measured THz scattering data (see Sec. 4). To maximize THz scattering, the polarization of THz electric field was along the filament propagation axis.

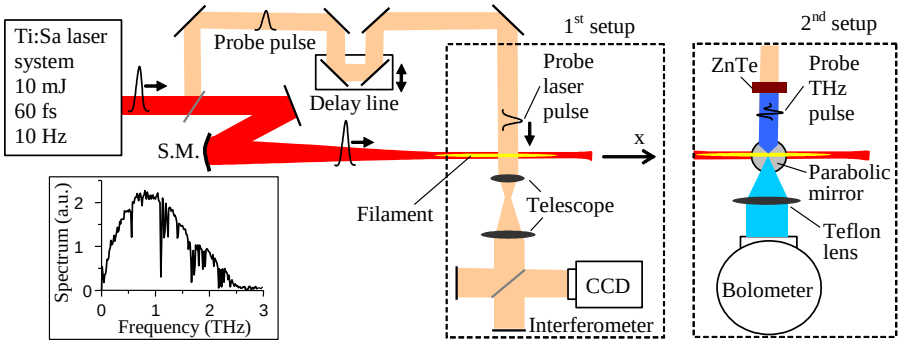

Fig. 1. Schematics of the experimental setups. Inset: the THz field spectrum generated in ZnTe crystal in the second setup.

3. Interferometric measurements of plasma density

Typical plasma density (~10^{16} - 10^{17} cm^{-3}) and diameter (~100-200 μm) of a filament in air [1, 2] lead to extremely small shifts of interference fringes in transverse optical interferometry (1st setup in Fig. 1). To measure the corresponding small phase shifts (~0.01 rad), the following procedure was used. The interferometric images with and without pump pulse were obtained. Image with the pump pulse (informative image) contained information about the plasma filament, while the image without pump pulse (background image) contained information about phase noise. For each informative image several (about 50) background images were taken. By applying the 2D FFT technique [8] phase maps for both informative and background interferometric images were obtained. After that each of 50 background phase maps were subtracted from the informative phase map and a selection of about ten phase maps with the minimal phase noise was made. The resulting phase map was obtained by averaging over this selection. To derive the transverse plasma density profile from the resulting phase-shift map we averaged the transverse phase-shift distribution along the filament, symmetrized the distribution relative to its center and then applied the inverse Abel transform. To minimize noise, high frequency spatial harmonics were filtered out.

Figure 2(a) shows the phase-shift map of the filament front edge (the laser pulse propagates from the left to the right, pulse energy W_0 = 5.4 mJ). The transverse phase shift distribution averaged along the filament ($0 < x < 300$ μm) and the corresponding radial distribution of electron density are shown in Figs. 2(b) and (c), respectively. Maximal phase shift in plasma is ~0.03 rad [Fig. 2(b)]. Plasma filament has a maximum plasma density N_{e0} of about 10^{17} cm^{-3} and FWHM diameter D_{FWHM} ~120 μm. The shape of the radial distribution can be fitted by a super-Gaussian function $\exp[-(r/r_0)^n]$ with $n \approx 5$ and $r_0 \approx 63$ μm. The value of the filament diameter agrees well with fluorescence image data measured by a CCD camera.

The dependence of plasma density and diameter of the plasma channel on distance along the filament is shown in Figs. 3(a) and 3(b) (data in Fig. 2 correspond to x = 0 in Fig. 3). After the onset of the filament at $x \approx -10$ mm the plasma density and the diameter grow sharply and reach the maximum values of ~9×10^{16} cm^{-3} and 120-140 μm, respectively. Further, the density maximum decreases slowly with ~2-fold decrease in diameter. According to Fig. 3, plasma channel length exceeds 4 cm for 5.4 mJ pulse energy. This agrees with the visible plasma channel length of about 5-7 cm at this energy.

#142643 - $15.00 USD Received 15 Feb 2011; revised 12 Mar 2011; accepted 14 Mar 2011; published 24 Mar 2011

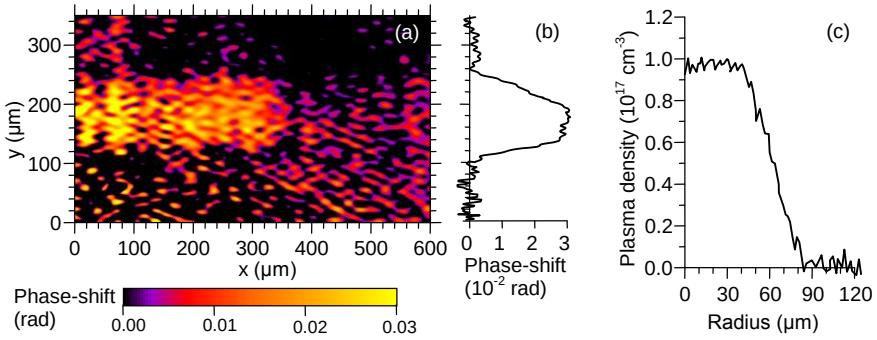

Fig. 2. (a) Phase shift map at the front edge of the filament (W_0 = 5.4 mJ.). (b) Phase shift averaged along the filament. (c) Transverse profile of electron density.

The energy dependence of plasma density N_{e0} and diameter of the plasma filament at x = 0 is presented in Figs. 4(a) and 4(b); x = 0 corresponds approximately to the center of the filament for W_0 = 5.4 mJ (point C in the inset in Fig. 4) and is ~3 cm closer to the spherical mirror as compared to the linear focus (point B). At x = 0 the probe pulse traverses the filament. Note that with increasing or decreasing pump energy, the position of the filament onset (point A) moves to or from the spherical mirror, respectively, while the rear edge of the filament stays near the linear focus [9]. Hence, with increasing pump energy, the probe pulse at the point C senses the onset (at W_0 ~4 mJ), the center (at W_0 ~5-6 mJ) and the rear edge of the filament (for W_0 ~7 mJ, when the filament has visible length ~10 cm), respectively. According to Fig. 4, both the plasma density and the diameter of the filament at the point C increase rapidly near W_0 = 4 mJ and reach 10^{17} cm^{-3} and 130 μm, respectively. Further increase of the pump energy leads to slow decrease of the plasma density at the point C while the plasma diameter increases to ~160 μm for W_0 = 7 mJ.

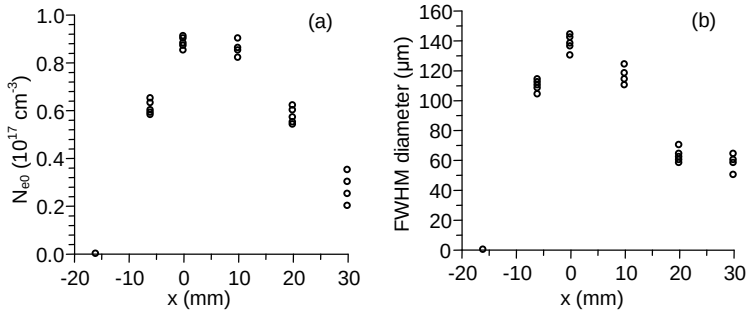

Fig. 3. (a) Maximum plasma density N_{e0} and (b) FWHM diameter of the plasma channel along the filament. The pump pulse energy is W_0 = 5.4 mJ.

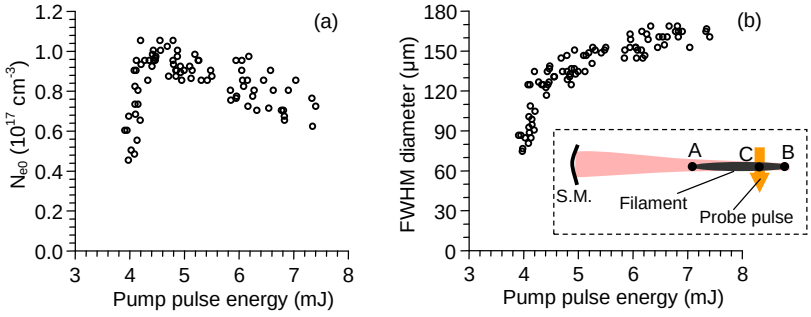

Fig. 4. (a) Plasma density N_{e0} and (b) FWHM diameter of the filament as a function of the pump pulse energy W_0. Inset – the geometry of energy dependence measurements (see text).

#142643 - $15.00 USD Received 15 Feb 2011; revised 12 Mar 2011; accepted 14 Mar 2011; published 24 Mar 2011

An asymmetric shape of plasma transverse phase shift distribution was observed for pulse energies exceeding ~7.5 mJ. This can be due to the beginning of multifilamentation. For some pulses asymmetric phase shift distributions were obtained for energy less than 7 mJ.

Plasma density decay was measured by scanning the time delay of the probe pulse (Fig. 5). Electron density decreases rapidly (from 0.9×10^{17} cm^{-3} to ~0.2×10^{17} cm^{-3}) within 300 ps. The transverse distribution of the electron density (Fig. 5(b)) flattens during the decay. This observation demonstrates nonlinear character of the electron relaxation: higher electron density relaxes faster. For t > 300 ps the interferometric images became too noisy and the terahertz scattering technique was employed.

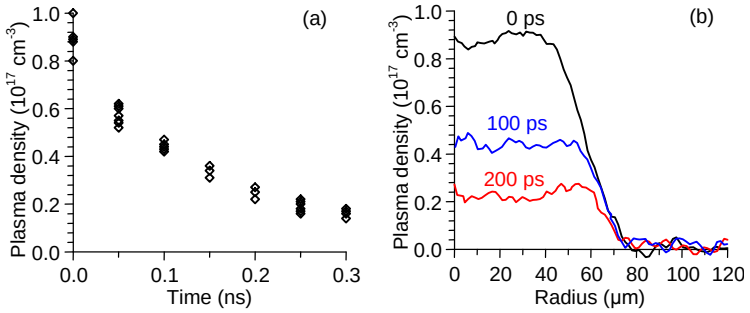

Fig. 5. (a) Plasma density decay at x = 0, W = 5.4 mJ. (b) Transverse plasma density distributions for t = 0 ps, 100 ps and 200 ps.

4. Terahertz measurement of plasma decay dynamics

For terahertz radiation (0.3-3 THz) a critical plasma density lies in the range 10^{15}-10^{17} cm^{-3}. Thus, scattering of THz radiation from the plasma filament with transverse diameter comparable to THz wavelength is very sensitive to the value of the electron density in this range. Following this idea, we investigated plasma decay by measuring the scattering of the probe THz pulse as a function of time delay by the bolometer (Fig. 6(a)).

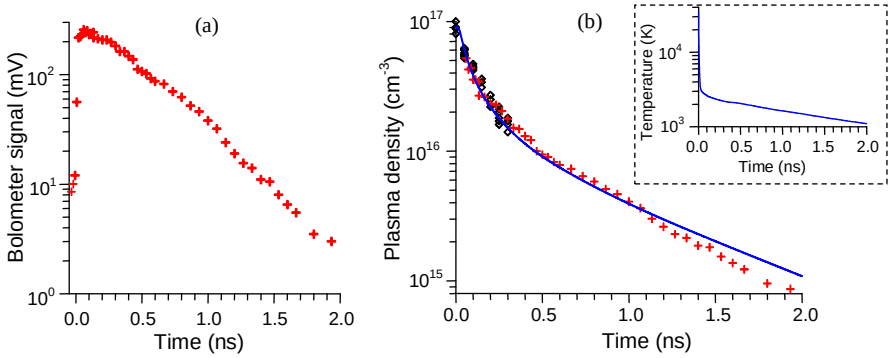

Fig. 6. (a) Bolometer signal as a function of time delay. (b) Plasma density N_{e0} decay. Crosses and diamonds – terahertz and interferometric experimental measurements, respectively. Solid curve – theoretical calculation. Inset – electron temperature as a function of time.

In Fig. 6(a) the rapid increase of the bolometer signal at t ≈0 is caused by the terahertz scattering from the beginning of the filament. Duration of the growing part of the signal (~10 ps) corresponds to the propagation time of the pump laser pulse through the ~4 mm diameter THz beam. During the next 200 ps the THz signal does not change significantly, while the plasma density decreases 4-5 times according to the interferometric measurements. This effect is explained by saturation of the detected THz energy scattered from the overcritical plasma. Indeed, the bolometer has maximum detection frequency ~1.5 THz which corresponds to ~3×10^{16} cm^{-3} critical plasma density. Hence, the scattered THz radiation practically does not

#142643 - $15.00 USD Received 15 Feb 2011; revised 12 Mar 2011; accepted 14 Mar 2011; published 24 Mar 2011

sense changes of the plasma density above 3×10^{16} cm^{-3}. According to interferometric measurements, plasma density reached 3×10^{16} cm^{-3} at 200 ps. Thus, terahertz signal should start to decrease only for $t > 200$ ps and exactly this was observed in experiment (Fig. 6(a)). We measured plasma decay up to 2 ns. This maximum time was limited by bolometer sensitivity.

To calculate plasma density N_{e0} from the scattered THz signal, a numerical code calculating radiation scattering by axial symmetric cylinder with arbitrary transverse distribution of electron density was developed. For solution of the inverse problem (for finding plasma density N_{e0} from the THz pulse scattering) we used interferometric data on the transverse distribution and absolute value of electron density at $t = 200$ ps [see Fig. 5(b)]. The result of plasma density calculation acquired from THz scattering data is shown in Fig. 6(b) by crosses (diamonds – interferometric data). According to Fig. 6(b), interferometric and terahertz scattering results agree well in the region of overlap. As follows from Fig. 6(b) plasma density decreases two orders of magnitude (from ~10^{17} cm^{-3} to 10^{15} cm^{-3}) on a time scale of 2 ns.

5. Numerical simulation of plasma decay

The detailed analysis has shown that among numerous plasma chemical reactions possible in atmospheric air [10] only several processes make a significant contribution to plasma density decay after filament formation (over the time period of 2 ns). The reactions included in our calculation are listed in Table 1. Five channels of electron recombination were taken into account: dissociative and three-body electron recombination with O_2^+ (reactions 1 and 2, respectively) and dissociative electron recombination with complex ions $N_2O_2^+$, O_4^+, and $H_2O{\cdot}O_2^+$ (reactions 3, 4, and 5) formed in reactions 6–11. We used the relative humidity 50% in our calculations. Note that electron attachment to O_2 molecules plays a minor role on our time scale and was not considered in our calculation.

Table 1. Reactions for Plasma Decay Calculation.

No	Reaction	Rate coefficient
1	$e^- + O_2^+ \rightarrow O + O$	$1.95{\cdot}10^{-7}{\cdot}(300/T_e)^{0.7}$ cm^3/s.[11,15]
2	$e^- + e^- + O_2^+ \rightarrow O_2 + e^-$	$6.1{\cdot}10^{-20}{\cdot}(300/T_e)^{9/2}$ cm^6/s [12]
3	$e^- + N_2O_2^+ \rightarrow N_2 + O_2$	$1.3{\cdot}10^{-6}{\cdot}(300/T_e)^{1/2}$ cm^3/s [10]
4	$e^- + O_4^+ \rightarrow O_2 + O_2$	$4.2{\cdot}10^{-6}{\cdot}(300/T_e)^{1/2}$ cm^3/s [15]
5	$e^- + H_2O{\cdot}O_2^+ \rightarrow O_2 + H_2O$	$2{\cdot}10^{-6}{\cdot}(300/T_e)^{1/2}$ cm^3/s [13]
6	$O_2^+ + 2N_2 \rightarrow N_2O_2^+ + O_2$	$0.9{\cdot}10^{-30}{\cdot}(300/T)^2$ cm^6/s [10]
7	$N_2O_2^+ + N_2 \rightarrow 2N_2 + O_2^+$	$1.1{\cdot}10^{-6}{\cdot}(300/T)^{5.3}e^{-2357/T}$ cm^3/s [10]
8	$O_2^+ + 2O_2 \rightarrow O_4^+ + O_2$	$2.4{\cdot}10^{-30}{\cdot}(300/T)^{3.2}$ [10]
9	$O_4^+ + O_2 \rightarrow O_2^+ + 2O_2$	$3.3{\cdot}10^{-6}{\cdot}(300/T)^4e^{-5030/T}$ cm^3/s [10]
10	$N_2O_2^+ + O_2 \rightarrow O_4^+ + N_2$	10^{-9} cm^3/s [10]
	$H_2O + O_2^+ + M \rightarrow H_2O{\cdot}O_2^+ + M$	
11	$M = O_2, N_2$	$0.6{\cdot}10^{-28}$ cm^6/s [13]

According to Table 1, the rate coefficients strongly depend on electron temperature T_e. We assumed the initial electron temperature to be 3 eV, which corresponds to the electron quiver energy in the pump laser pulse. The temporal evolution of T_e was calculated from a numerical solution of the electron energy conservation equation [13]. The frequency of electron energy relaxation in collisions with molecules was obtained using the computer code [14]. This code solves the Boltzmann equation for electrons taking into account electron energy losses due to electronic, vibrational and rotational excitation of N_2 and O_2, and elastic scattering of electrons by charged particles and molecules. Electron gas heating in three-body recombination [13] was taken into account, but heating in dissociative recombination was found to be negligible. Due to high electron-electron collision frequency at high ionization degree in our experiment the electron energy distribution function was assumed to be Maxwellian. The gas temperature was assumed to be 293 K. The calculated electron

#142643 - $15.00 USD Received 15 Feb 2011; revised 12 Mar 2011; accepted 14 Mar 2011; published 24 Mar 2011

temperature is shown in the inset in Fig. 6(b). According to our analysis, the fast (within several tens of ps) temperature decrease to ~3000 K results from electronic and vibrational excitation of molecules. With a further temperature decrease rotational excitation dominates.

The time evolution of the electron density (solid curve in Fig. 6(b)) was calculated on the basis of the reactions listed in Table 1 and the calculated electron temperature. Good agreement is observed between the experimental results and the calculations. It follows from our calculations that during the first ~1 ns the reactions of dissociative and three-body recombination with O_2^+ ion (reactions 1 and 2) play the main role in plasma density decrease. On the larger time scale, recombination with complex ions (reactions 3, 4, and 5) dominate. Yet, all the five channels of electron losses are important to assure a qualitative agreement with the experimental data.

5. Conclusion

To conclude, the transverse distribution of electron concentration with maximum plasma density of ~10^{17} cm^{-3} in a single plasma filament was measured by the direct method of transverse interferometry. The detailed investigation of plasma decay was performed using a combination of the interferometry and terahertz scattering techniques. Fast decay of plasma density by two orders of magnitude within 2 ns was observed. The theoretical model accounting for dissociative and three-body electron recombination with simple and complex positive ions, collisional cooling and recombination heating of electrons adequately describes the measured plasma decay dynamics.

Acknowledgments

This work was supported in part by the Federal Program of the Russian Federation "Research and education specialists of innovative Russia" (No П948) and the Russian Foundation for Basic Research (grants Nos. 09-02-12324 and 09-02-01359). S.B.B. and M.V.T. also acknowledge partial support from the Presidential Grant MK-4506.2010.2.

#142643 - $15.00 USD Received 15 Feb 2011; revised 12 Mar 2011; accepted 14 Mar 2011; published 24 Mar 2011